

# Hadron structure for $x \ll 1$ and upcoming collider measurements\*

*F. Hautmann*

*Theoretical Physics Department, University of Oxford, Oxford OX1 3NP*

Abstract

We discuss theoretical aspects of parton distribution functions for very high energy scattering in relation with upcoming measurements in DIS and hadron-hadron collisions.

## 1 Introduction

The Large Hadron Collider will operate with very high parton luminosities. As these rise steeply for decreasing momentum fraction  $x$ , a large number of events sample gluon and sea-quark distributions at  $x \ll 1$ . Understanding the theoretical accuracy in the determination of these distributions is relevant both to obtain reliable predictions for cross sections of hard processes and to investigate new aspects of QCD physics at very small  $x$ .

Current determinations of parton distribution functions for  $x \lesssim 10^{-2}$  largely depend on deep inelastic scattering data. We start the discussion in Sec. 2 by commenting on such determinations, with a view in particular to the forthcoming longitudinal structure function measurements.

Most of the phenomenological pdf analyses place cuts on the low- $Q^2$  region, in order to ensure the applicability of perturbation theory. However, a lot of the experimental information on  $x \ll 1$  physics lies at present with data that involve scales of few GeV. In Sec. 3 we turn to discuss how s-channel methods, designed to describe high-energy scattering down to lower and lower  $Q^2$ , might be used in the context of the parton picture. Measurements of jet production in the DIS current fragmentation

---

\*Presented at the IX Workshop on Nonperturbative QCD, IAP, Paris, 4-8 June 2007.

and central region could be exploited in this framework to extract information on the nonperturbative parameters of multiple parton scattering.

We illustrate in Sec. 4 the use of the above methods for estimating power corrections to structure function's evolution from multiple scattering. We emphasize the distinctive behavior of the results in the region of intermediate scales just above 1 GeV. Through momentum sum rules and evolution, the low- $x$  and low- $Q^2$  region may affect predictions for processes at much higher  $x$  and higher mass scales. Some additional comments on related issues are given in Sec. 5. We conclude in Sec. 6.

## 2 Flavor-singlet parton evolution

Present determinations of parton distribution functions are based on fits to available collider data [1, 2, 3, 4], using renormalization-group evolution equations to connect measurements at different mass scales  $\mu$ . The region  $x \ll 1$  is dominated by flavor-singlet evolution,

$$\frac{d}{d \ln \mu^2} \begin{pmatrix} f_S \\ f_g \end{pmatrix} = \begin{pmatrix} P_{qq} & P_{qg} \\ P_{gq} & P_{gg} \end{pmatrix} \otimes \begin{pmatrix} f_S \\ f_g \end{pmatrix} , \quad (1)$$

where  $f_g$  and  $f_S$  are the gluon and sea-quark distributions, and  $P_{ij}$  is the perturbatively calculable evolution kernel. The  $f_g$  distribution in the range  $x \lesssim 10^{-2}$ , in particular, is relevant for measurements of production processes dominated by gluon fusion at the LHC, including heavy flavor production [5, 6, 7] and Higgs boson production [6, 8].

At present the extraction of  $f_g$  at  $x \lesssim 10^{-2}$  depends on DIS data for the  $Q^2$  derivative of the structure function  $F_2$  ( $\dot{F}_2 = dF_2/d \ln Q^2$ ),

$$F_2 \sim f_S , \quad \dot{F}_2 \sim P_{qg} \otimes f_g [1 + \mathcal{O}(\Lambda^2/Q^2)] + \text{quark term} . \quad (2)$$

The kernel  $P_{ij}$  used for standard pdf determinations is evaluated in fixed order of perturbation theory (NLO and, in some of the analyses now becoming available [1, 3], NNLO). As indicated by Eq. (2), however, the extraction of  $f_g$  is especially sensitive to higher-loop corrections to the gluon  $\rightarrow$  quark splitting kernel  $P_{qg}$ . In particular, for  $x \ll 1$  logarithmically enhanced contributions  $\alpha_s^{k+1} x^{-1} \ln^{k-1} x$  [9] to  $P_{qg}$  are present for any  $k \geq 1$ , and need to be resummed. The numerical impact of terms of this type on the global fits is examined e.g. in [4].

While the summation of  $\ln x$  terms in the pure-gluon sector has been studied extensively for quite some time (see reviews in [6, 10], and references therein), only recently have the first analyses appeared [11, 12, 13] that implement both gluon [14] and quark [15] next-to-leading  $\ln x$  corrections to the matrix kernel  $P_{ij}$ . This is theoretically appealing, as quark corrections are required in order to merge consistently the  $x \rightarrow 0$  expansion with the short-distance behavior and the renormalization group,

and opens the possibility for resummed analyses to become directly relevant to phenomenology.

The production of  $b$ -quarks at the LHC will be sensitive to  $f_g$  at  $x \lesssim 10^{-2}$ . Recall that the theoretical uncertainties on NLO predictions for the  $b$  cross sections, while on the order of a few ten percent at the Tevatron [16], increase to well over a factor of 2 at LHC energies [5, 7, 16]. Improving upon present predictions will likely involve a variety of physical effects, from higher-loop corrections beyond NLO to nonperturbative processes both in the initial and the final states. An improved treatment of  $x \rightarrow 0$  contributions for both the pdfs and the short-distance cross sections should help understand the sources of the large uncertainties at the LHC, and possibly reduce them.

The production of Higgs bosons may also receive sizeable contributions from low- $x$  gluon events at the LHC, depending on the Higgs mass range and the kinematical region in the Higgs rapidity and  $p_T$ . See e.g. [17] for studies of high-energy effects on the accuracy of Higgs boson cross sections.

The  $x \ll 1$  region will be probed experimentally by the forthcoming measurements of the longitudinal structure function  $F_L$  [18]. A recent phenomenological study of  $F_L$  may be found in Ref. [12]. This presents a thorough comparison of fixed-order predictions through NNLO [19] and predictions including the  $\ln x$  resummation for the  $F_L$  coefficient functions [15]. The analysis [12] shows that i) the NLO and NNLO corrections to  $F_L$  are large, as observed in [19], and lead to strong instabilities causing perturbation theory to be badly behaved at low  $x$ ; ii) resummed results improve this behavior, and allow one to obtain more reliable theoretical predictions throughout a wider range in the kinematical variables. This is potentially significant, since the  $F_L$  measurements will provide an independent observable, to be combined with  $\dot{F}_2$ , to perform a complete flavor-singlet analysis and probe the accuracy of the theory at  $x < 10^{-2}$  more stringently than ever so far.

A different, but possibly related issue concerns the initial conditions at low mass scales for pdf evolution. Working to NNLO, Ref. [20] observes that rather different features than in [12, 19, 21] are obtained in the fixed-order predictions for  $F_L$  if different assumptions are made [20, 22] for the initial conditions. We note that this marked dependence on the initial condition may be related to using a fixed-order truncation of perturbation theory that is not well-behaved at low  $x$ , and could likely be reduced in the improved theory including resummation.

On the other hand, while resummed evolution schemes provide better theoretical control on the  $x \ll 1$  region [11, 12, 13], note that the coefficients themselves of resummed perturbation theory signal the onset of dynamics beyond the  $\alpha_s$  expansion. One way to see this is to examine the singularity structure of resummed coefficients in the plane of the effective  $x \rightarrow 0$  anomalous dimension  $\gamma_\omega(\alpha_s)$  [23]. The strong branch-point singularities in gluon-channel coefficients [23]  $R_\omega(\alpha_s) \sim 1/\sqrt{1/2 - \gamma_\omega(\alpha_s)}$ , with  $\gamma_\omega \rightarrow 1/2$  for  $x \rightarrow 0$ , imply that effects beyond the perturbation expansion are to be

included in order to fully describe the high-energy limit (see also discussion in [24]).

In Eq. (2) we have indicated explicitly contributions to  $\hat{F}_2$  suppressed by powers of  $1/Q^2$ . Because present DIS data that are relevant to extract the gluon density for  $x < 10^{-2}$  do not have very high  $Q^2$ , these power corrections may be expected to have non-negligible effects on the estimate of the theoretical accuracy on pdf's for the LHC. In the next sections we turn to methods for the subset of power-like contributions that comes from graphs with multiple gluon scatterings.

### 3 Relating parton approach and s-channel approach

Methods to take account of multiple scatterings are based on the s-channel picture of deep inelastic collisions. See [25] for an introduction to the physical picture, and [26, 27, 28, 29] for motivation from high-density QCD. The main advantage of this approach is that it gives a formulation that can be used down to small  $Q^2$ , incorporating nonperturbative physics at very high energies in Wilson-line operator matrix elements.

The s-channel approach leads to a different picture of the hard collision than the parton approach, as it works in a different reference frame, and uses different degrees of freedom. Nevertheless, the two pictures are not incompatible. In the region where their domains of validity overlap, they must describe the same physics. Ref. [30] presents a framework to connect the two pictures.

The method [30] is based on constructing explicitly an s-channel representation for the renormalized parton distribution function in terms of Wilson-line matrix elements. In this representation the quark distribution  $f_q$  is given by the coordinate-space convolution (Fig. 1)

$$xf_q(x, \mu) = \int dz \int d\mathbf{b} u(\mu, \mathbf{z}) \Xi(\mathbf{z}, \mathbf{b}) - UV \quad , \quad (3)$$

where  $\Xi$  is the hadronic matrix element of eikonal-line operators,

$$\begin{aligned} \Xi(\mathbf{z}, \mathbf{b}) &= \int [dP'] \langle P' | \frac{1}{N_c} \text{Tr} \{ 1 - V^\dagger(\mathbf{b} + \mathbf{z}/2) V(\mathbf{b} - \mathbf{z}/2) \} | P \rangle \quad , \\ V(\mathbf{z}) &= \mathcal{P} \exp \left\{ -ig \int_{-\infty}^{+\infty} dz^- A_a^+(0, z^-, \mathbf{z}) t_a \right\} \quad , \end{aligned} \quad (4)$$

$\mathbf{z}$  is the transverse separation between the eikonal lines,  $\mathbf{b}$  is the impact parameter, and the function  $u(\mu, \mathbf{z})$  is evaluated explicitly in [30] at one loop using the  $\overline{\text{MS}}$  scheme for the renormalization of the ultraviolet divergences  $\mathbf{z} \rightarrow 0$ .

The convolution (3) expresses the fact that for  $x \ll 1$  the operator defining the quark distribution function creates the partonic system, made of a color-triplet eikonal line and an antiquark, at large longitudinal distances  $y^- \approx 1/(xP^+)$  far outside the

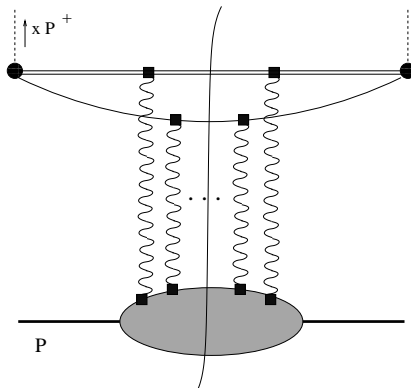


Figure 1: Quark distribution function in the s-channel picture.

target [25]. The  $\overline{\text{MS}}$  result [30] can be recast in a physically more transparent form in terms of a cut-off on the  $\mathbf{z}$  integration region (see also [31]), as long as the scale  $\mu$  is sufficiently large compared to the inverse hadron radius:

$$x f_{q/p}(x, \mu) = \frac{N_c}{3\pi^4} \int d\mathbf{b} \frac{d\mathbf{z}}{z^4} \theta(\mathbf{z}^2 \mu^2 > a^2) \Xi(\mathbf{z}, \mathbf{b}) \quad , \quad (5)$$

where  $a$  is a renormalization scheme dependent coefficient [30],

$$a = 2e^{1/6-\gamma} \approx 1.32657 \quad , \quad (6)$$

with  $\gamma$  the Euler constant. The Wilson-line matrix element  $\Xi(\mathbf{z}, \mathbf{b})$  receives contribution from both long distances and short distances. At small  $\mathbf{z}$  it can be treated by a short distance expansion. By using renormalization-group evolution equations, the leading term in the expansion can be related to a well-defined integral of the gluon distribution function [30]. At large distances  $\mathbf{z}$ ,  $\Xi$  has to be fit to data, or parameterized by models consistently with bounds from unitarity and saturation [29, 36].

Besides parton distribution functions, the s-channel representation discussed above is potentially interesting for jet production. To this end, we note that Eqs. (3),(5) imply introducing a cut-off in rapidity [30] in order to separate slow and fast partons in the picture of Fig. 1, and to factor out the Wilson-line matrix element. The dependence on the method of carrying out this separation enters in higher orders for the quark distribution, and in leading order for the gluon. Both the quark and the gluon channel contribute to the jet structure of the final states. Nevertheless, if one considers jet cross sections by fixing e.g. the total minus momentum of the dijet system, the sensitivity to the rapidity cut-off is suppressed, as long as the jets are produced sufficiently far from the fragmentation region of the target. Then the application of the s-channel method to measurements of jet production will give rather direct information on the contribution of multiple parton scatterings.

Note that current shower Monte-Carlo generators include model parameterizations of multiple interactions in order to produce realistic event simulations, see e.g. [32, 33]. In this respect, jet rapidity distributions in the DIS current fragmentation and central regions, once analyzed using the s-channel picture, are potentially useful in order to constrain the nonperturbative parameters of such models.

The physical picture described in this section relies on the large separation in lightcone coordinate between creation of the partonic system and interactions with the target. This separation is of order a hundred fermi in the proton rest frame for  $x \lesssim 10^{-2}$  (see remark after Eq. (4)). The condition for the applicability of the approach is satisfied in the case of high-energy collisions of large nuclear targets as well. The approach should be relevant for the physics of high- $p_t$  probes in heavy ion collisions at the LHC and of nuclear parton distributions [34].

## 4 Power corrections from the s-channel

The representation (3), evaluated in a well-prescribed renormalization scheme, is the key ingredient that allows one to relate [30, 35] results of s-channel calculations for structure functions [26, 29, 36] to the OPE factorization,

$$F_2 = C \otimes f + \frac{1}{Q^2} C^{(4)} \otimes f^{(4)} + \dots \quad , \quad (7)$$

and, in particular, to identify power-suppressed contributions to the  $Q^2$  evolution of  $F_2$  of the form

$$\dot{F}_2 \simeq P_{qg} \otimes f_g [1 + \delta] + \text{quark term} \quad , \quad \delta \simeq \sum_{k \geq 1} a_k \left( \alpha_s \frac{1}{x^\beta} \frac{\Lambda^2}{Q^2} \right)^k \quad . \quad (8)$$

The enhanced  $x \rightarrow 0$  behavior in the power correction  $\delta$  in Eq. (8) is produced from graphs with multiple gluon scatterings, and is consistent with observations of approximate geometric scaling in low-x data [37].

Refs. [35, 38] introduce moments  $\lambda^2$  of the matrix element  $\Xi$  in Eq. (4),

$$\lambda^2(-v) = \frac{1}{\Gamma(v)} \int \frac{dz}{\pi z^2} (z^2)^{v-1} \int d\mathbf{b} \Xi(\mathbf{z}, \mathbf{b}) \quad , \quad (9)$$

and express the  $1/(Q^2)^k$  correction in terms of  $\lambda^2(k)$  times coefficients computable as functions of  $\alpha_s$ ,  $x$  and  $\ln Q^2$ , schematically in the form

$$\frac{dF_2}{d \ln Q^2} = \left( \frac{dF_2}{d \ln Q^2} \right)_{\text{LP}} + \sum_{k=1}^{\infty} R_k \frac{\lambda^2(k)}{(Q^2)^k} \quad . \quad (10)$$

The first term in the right hand side is the leading-power parton result, and the moments  $\lambda$  in the subleading terms are dimensionful nonperturbative parameters, to be determined from comparison with experimental data. Observe that any number of rescatterings contribute to the moment  $\lambda^2(k)$  through the eikonal operators (4). Thus the correction of order  $1/(Q^2)^k$  receives contribution from the exchange of arbitrarily many gluons. This is characteristic of the small- $x$  power correction and can be contrasted with counting rules arguments, valid at large  $x$ , that link the power in  $Q^2$  with the number of parton lines exchanged in the t-channel.

The result of determining the nonperturbative  $\lambda$  parameters from  $F_2$  data [39] at both low and high  $Q^2$  is shown in Fig. 2 in the left hand side plot [35]. The corresponding power correction is plotted on the right hand side of Fig. 2. Here the correction is normalized to the full answer and multiplied by  $-1$ .

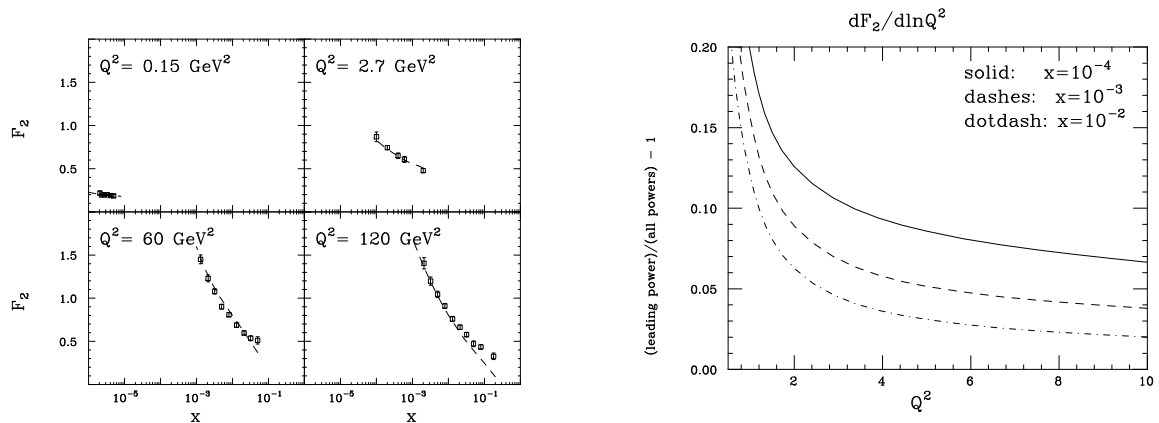


Figure 2: (left) The result of fitting the  $\lambda^2$  parameters to the data[39]; (right) power corrections to  $dF_2/d\ln Q^2$  versus  $Q^2$  at different values of  $x$ [35].

The analysis [35] indicates that with physically natural choices of the parameters in the nonperturbative matrix elements in Eqs. (4),(9) one can achieve a sensible description of data for  $x < 10^{-2}$  in a wide range of  $Q^2$  and still have moderate power corrections to  $dF_2/d\ln Q^2$ . Corrections turn out to be negative and below 20 % for  $x \gtrsim 10^{-4}$  and  $Q^2 \gtrsim 1 \text{ GeV}^2$ . This observation suggests that the power expansion is not breaking down, and should still work at least to the values of  $x$  considered in Fig. 2.

However, we also see from Fig. 2 that for small  $x$  the corrections fall off slowly in the region of medium  $Q^2$ ,  $Q^2 \simeq 1 - 10 \text{ GeV}^2$ , behaving effectively like  $1/Q^\nu$  with  $\nu$  close to 1 [35]. For instance, one has  $\nu \simeq 1.2$  for the curve  $x = 10^{-3}$  in the right-hand side plot of Fig. 2. As a consequence of the slowly decreasing behavior, the power corrections stay on the order of 10% up to  $Q^2$  of a few  $\text{GeV}^2$  for  $x \lesssim 10^{-3}$ . This slow fall-off differs from parameterizations of higher twist commonly used in global

analyses (see e.g. Ref. [4]), and may be relevant for phenomenology as it affects the medium  $Q^2$  region of the data that are useful to extract  $f_g$  at low  $x$ .

## 5 Further comments

The region of low  $x$  and low-to-medium  $Q^2$  influences predictions at much higher  $x$  and mass scales through momentum sum rules and evolution. We give below some further comments.

It is worth noting that the biggest contribution to the power correction to  $\dot{F}_2$  in [35] comes from the longitudinal component. The derivative  $dF_T/d\ln Q^2$  has smaller power corrections than  $dF_2/d\ln Q^2$ . This provides additional motivation for the separate measurement of  $F_L$  [18]. Similar conclusions are reached from a different perspective based on the fits [4, 21], investigating the effect of power-like terms on global analyses at both high  $x$  and low  $x$ . (These fits also include parameterizations of power effects from self-energy graph insertions. We recall here that only relatively few results are known as yet on such effects in flavor-singlet observables. See [40] for a recent study, and early discussions in [41].)

The curves in Fig. 2 are obtained using NLO parton distributions. It is natural to expect a change in the power correction when going from NLO to NNLO. We note that the decrease in the low- $x$  gluon at NNLO [3] is consistent with the possibility that NNLO partons give smaller power corrections.

Observe that in the calculation described in Sec. 4 the slow fall-off with  $Q^2$  results from summing the terms proportional to the moments  $\lambda$  in Eq. (9). These in turn are obtained from expanding the s-channel answer in powers of  $1/Q^2$ , and enforcing consistency with the standard parton framework. It will be of interest to compare the  $Q^2$  behavior found here with the behavior due to the anomalous dimensions that result from nonlinear evolution equations such as those, e.g., used in [26, 27, 28, 40].

It will also be of interest to investigate the relation of the result (9),(10) for the power correction with the  $x$ -rescaling form proposed in [42] and applied to nuclear targets. This should likely involve the finite lightcone-time cut-off that enters in the high-energy eikonal approximation (see e.g. [43]), reflecting the fact that the eikonalized projectile-target interactions do not spread out to arbitrarily large times in the far past and the far future.

The behavior observed in Fig. 2 suggests that the power corrections may be characterized by a nonperturbative scale substantially larger than  $\Lambda_{\text{QCD}}$ . It is possible that this can be related to the dynamical cut-off on large transverse distances  $\mathbf{z}$  imposed by unitarity requirements (“black disc” limit) on the correlator  $\Xi$  in Eq. (4). To pursue this, further studies of the moments (9) are warranted. Also, the analogue of these moments for eikonal operators (4) in the adjoint representation will be relevant for processes coupled directly to the gluon distribution. An especially interesting case



is that of diffractive DIS events [44], where cross sections depend quadratically on the  $\Xi$  correlator, and gluonic contributions typically dominate quark contributions by one order of magnitude. See comments in [38], and references therein, on the possible role of the “blackness” cut-off in hard-diffractive data.

## 6 Conclusion

The partonic structure of protons and nuclei will be probed for small values of  $x$  at the LHC. DIS measurements of longitudinal  $F_L$ , expected in the coming year, will provide very valuable, new experimental input. As discussed in Sec. 2, improved theoretical tools for the evolution of parton distributions are starting to become available that include the results of next-to-leading  $\ln x$  resummation for both gluon *and* quark channels, as is required by consistency with the short-distance behavior and the renormalization group.

Much of the present information on the region  $x < 10^{-2}$  comes from deep inelastic data involving scales of few GeV. Physics beyond the perturbation expansion is likely to play a role in this regime. The physical picture of hard collisions that is designed to go down to lower and lower  $Q^2$  when  $x$  is small is the s-channel picture. A method to use results of s-channel calculations in the context of the parton framework is discussed in Sec. 3, and applied in Sec. 4 to corrections to structure function’s evolution suppressed by powers of  $1/Q^2$  but enhanced as  $x \rightarrow 0$ .

The results presented build a physical picture of the sea-quark distribution for very high energies, that allows one to discuss quark saturation. Nonperturbative power-like effects are expressed in terms of moments of Wilson-line eikonal correlators. The picture suggests the possibility of using measurements of jet lepton production in the intermediate rapidity region to measure effects of parton rescatterings.

**Acknowledgments.** I thank the workshop’s organizers and staff for the kind invitation. I thank D. Soper for discussions and for careful reading of the manuscript.

## References

- [1] S. Alekhin, K. Melnikov and F. Petriello, Phys. Rev. D **74** (2006) 054033; S. Alekhin, JETP Lett. **82** (2005) 628.
- [2] P.M. Nadolsky, H.-L. Lai, Q.-H. Cao, J. Huston, J. Pumplin, D. Stump, W.-K. Tung and C.-P. Yuan, arXiv:0802.0007; J. Pumplin, A. Belyaev, J. Huston, D. Stump and W.K. Tung, JHEP **0602** (2006) 032.
- [3] A.D. Martin, W.J. Stirling, R.S. Thorne and G. Watt, Phys. Lett. B **652** (2007) 292.

- [4] A.D. Martin, R.G. Roberts, W.J. Stirling and R.S. Thorne, *Eur. Phys. J.* **C35** (2004) 325.
- [5] J. Baines et al., Report of the Heavy Quark Working Group, hep-ph/0601164.
- [6] S. Alekhin et al., Proceedings of the Workshop “HERA and the LHC”, hep-ph/0601012.
- [7] P. Nason et al., Report on bottom production, in “SM physics (and more) at the LHC”, hep-ph/0003142.
- [8] M. Albrow et al., Tevatron-for-LHC Report of the QCD Working Group, FERMILAB-CONF-06-359 (2006), hep-ph/0610012.
- [9] S. Catani and F. Hautmann, *Phys. Lett. B* **315** (1993) 157; R.K. Ellis, F. Hautmann and B.R. Webber, *Phys. Lett. B* **348** (1995) 582.
- [10] J.R. Andersen et al., *Eur. Phys. J.* **C48** (2006) 53.
- [11] M. Ciafaloni, D. Colferai, G.P. Salam and A.M. Stasto, *JHEP* **0708** (2007) 046.
- [12] C.D. White and R.S. Thorne, *Phys. Rev. D* **75** (2007) 034005.
- [13] G. Altarelli, R.D. Ball and S. Forte, talk by G. Altarelli at the Conference RAD-COR2007, October 2007; arXiv:0802.0032.
- [14] V.S. Fadin and L.N. Lipatov, *Phys. Lett. B* **429** (1998) 127; G. Camici and M. Ciafaloni, *Phys. Lett. B* **430** (1998) 349.
- [15] S. Catani and F. Hautmann, *Nucl. Phys.* **B427** (1994) 475.
- [16] M. Cacciari, S. Frixione, M.L. Mangano, P. Nason and G. Ridolfi, *JHEP* **0407** (2004) 033.
- [17] S. Marzani, R.D. Ball, V. Del Duca, S. Forte and A. Vicini, arXiv:0801.2544; V. Del Duca, W. Kilgore, C. Oleari, C.R. Schmidt and D. Zeppenfeld, *Phys. Rev. D* **67** (2003) 073003; F. Hautmann, *Phys. Lett. B* **535** (2002) 159.
- [18] H1 Coll. (N. Raicevic for the collaboration), in Proceedings of the Workshop DIS2007, p. 293; Zeus Coll. (S. Shimizu for the collaboration), in Proceedings of the Workshop DIS2007, p. 289.
- [19] S. Moch, J.A.M. Vermaseren and A. Vogt, *Phys. Lett. B* **606** (2005) 123.
- [20] M. Glück, C. Pisano and E. Reya, arXiv:0711.1248.
- [21] A.D. Martin, W.J. Stirling and R.S. Thorne, *Phys. Lett. B* **635** (2006) 305.

- [22] M. Glück, C. Pisano and E. Reya, Eur. Phys. J. **C50** (2007) 29; M. Glück, E. Reya and A. Vogt, Eur. Phys. J. **C5** (1998) 461.
- [23] M. Ciafaloni and D. Colferai, JHEP **0509** (2005) 069; S. Catani, M. Ciafaloni and F. Hautmann, Phys. Lett. B **307** (1993) 147.
- [24] G. Camici and M. Ciafaloni, Phys. Lett. B **395** (1997) 118.
- [25] J.D. Bjorken, SLAC-PUB-6477 (1994); hep-ph/9610516.
- [26] Y. Hatta, E. Iancu and A.H. Mueller, JHEP **0801** (2008) 026.
- [27] Y.V. Kovchegov and H. Weigert, arXiv:0712.3732.
- [28] F. Gelis, T. Lappi and R. Venugopalan, Int. J. Mod. Phys. **E16** (2007) 2595.
- [29] K. Golec-Biernat, Nucl. Phys. **A755** (2005) 133; Acta Phys. Polon. **B35** (2004) 3103.
- [30] F. Hautmann and D.E. Soper, Phys. Rev. D **75** (2007) 074020.
- [31] F. Hautmann and D.E. Soper, arXiv:0712.0526, in Proceedings of the Conference PHOTON2007 (Paris, July 2007).
- [32] P. Bartalini, talk at Workshop on “QCD at Cosmic Energies”, ICTP, June 2007.
- [33] T. Sjöstrand and P.Z. Skands, Eur. Phys. J. **C39** (2005) 129; talks by T. Sjöstrand and by S. Gieseke at Workshop on Multiparton Interactions, Hamburg, May 2007.
- [34] See e.g. A. Accardi et al., Working Group report hep-ph/0308248, Workshop “Hard Probes in Heavy Ion Collisions at the LHC”; B. Müller, Nucl. Phys. **A783** (2007) 403; D. d’Enterria, Eur. Phys. J. **A31** (2007) 816.
- [35] F. Hautmann, Phys. Lett. B **643** (2006) 171.
- [36] A.H. Mueller, Nucl. Phys. **B558** (1999) 285; hep-ph/0111244, lectures at Cargese Summer School; J. Bartels, K. Golec-Biernat and H. Kowalski, Phys. Rev. D **66** (2002) 014001.
- [37] A. Stasto, K. Golec-Biernat and J. Kwiecinski, Phys. Rev. Lett. **86** (2001) 596.
- [38] F. Hautmann, arXiv:0706.3530, presented at the XLII Rencontres de Moriond, La Thuile, March 2007.
- [39] Zeus Coll., Eur. Phys. J. **C21** (2001) 443; Phys. Lett. **B487** (2000) 53.

- [40] E. Gardi, J. Kuokkanen, K. Rummukainen and H. Weigert, Nucl. Phys. **A784** (2007) 282.
- [41] Yu.L. Dokshitzer, hep-ph/9812252, in Proc. ICHEP98 (Vancouver); B.R. Webber, JHEP **9810** (1998) 012; F. Hautmann, Phys. Rev. Lett. **80** (1998) 3198.
- [42] J.W. Qiu and I. Vitev, Phys. Rev. Lett. **93** (2004) 262301.
- [43] F. Hautmann and D.E. Soper, Phys. Rev. D **63** (2000) 011501; F. Hautmann, Z. Kunszt and D.E. Soper, Nucl. Phys. **B563** (1999) 153; Phys. Rev. Lett. **81** (1998) 3333.
- [44] H. Abramowicz, talk at “HERA and the LHC” Workshop, Hamburg, March 2007; hep-ph/0001054, in Proc. Lepton-Photon Symposium (Stanford).